ACS OMEGA

http://pubs.acs.org/journal/acsodf

Article

Electrospun Carbon Nanofibers as an Electrochemical Immunosensing Platform for *Vibrio cholerae* Toxin: Aging Effect of the Redox Probe

Okoroike C. Ozoemena, Tobile Maphumulo, Jerry L. Shai,* and Kenneth I. Ozoemena*

Cite This: *ACS Omega* 2020, 5, 5762−5771

Read Online

ACCESS | Metrics & More | Article Recommendations | Supporting Information

ABSTRACT: An electrochemical immunosensor for *Vibrio cholerae* toxin (VCT) has been developed using electrospun carbon nanofibers (CNFs) as the electrode platform. To fabricate the immunosensor, the anti-cholera toxin antibody (Ab) was covalently immobilized on the electrode platforms using the carbodiimide chemistry for the amide bond formation. Every step of the formation of the immunosensor and the subsequent binding of the VCT subunit antigen (Ag) was electrochemically interrogated. The immunosensor gave excellent reproducibility and sensitivities: limits of detection (ca. 1.2×10^{-13} g mL^{-1}), limits of quantification (ca. 1.3×10^{-13} g mL^{-1}), and a wide linear range for the anti-cholera detection of 8 orders of magnitude (10^{-13} to 10^{-5} g mL^{-1}). One of the key findings was the enhanced sensitivity of the VCT detection using aged rather than the freshly prepared redox probe, described here as Redox Probe Aging-Induced Sensitivity Enhancement ("Redox-PrAISE"). The Redox-PrAISE was found more useful in the real application of these immunosensors, showing comparable or even better sensitivity for eight real cholera-infested water samples than the conventional clinical culture method. This immunosensor shows promise for the potential development of point-of-care diagnosis of VCT. Importantly, this study highlights the importance of considering the nature of the redox probe on the electrochemical sensing conditions when designing impedimetric immunosensors.

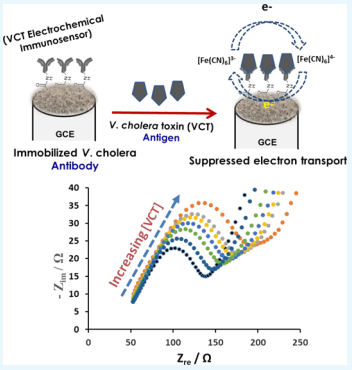

1. INTRODUCTION

Cholera is a major public health problem. It is caused by a bacterium called *Vibrio cholerae*, a gram-negative, facultative anaerobe. It is associated with several clinical symptoms, including diarrhea, vomiting, discomfort, cramping, sunken eyes, dry mouth, cold clammy skin, decreased skin turgor, and wrinkled hands and feet.[1−5] Cholera is known as a highly contagious disease capable of killing within hours if not identified and treated as the mortality rate can be more than 50% of the reported cases.[1] The most common transmission path is from person to person and from water sources or food to person due to poor sanitation and/or lack of access to clean water. It has been estimated by the World Health Organization (WHO) that there are more than 3−5 million cholera cases per year worldwide.[6] The disease affects mostly the resource-limited developing countries[6,7] and especially countries that frequently experience natural disasters, such as flooding, that lead to poor sanitation and/or lack of access to clean water. The incubation period of *V. cholerae* prior to the manifestation of symptoms may range from less than a day to five days.[2,3]

Considering the above-stated cholera-related health problems, there has always been an urgent need for the rapid diagnosis of cholera in order to expedite the treatment of affected individuals. The proper management of cholera outbreak requires affordable, accurate, reproducible, reliable, and rapid detection methods. It is well known that the early detection of cholera outbreak still remains a challenge.[8] There are several methods reported in the literature for the detection of cholera, as elegantly shown in a recent review.[9] The current methods as seen in the literature include the gold standard culture method,[10] enzyme-linked immunosorbent assay,[11] radioimmunoassay,[12] latex agglutination assays,[13] polymerase chain reaction (PCR),[5,14] and electrochemical techniques.[15−20] Generally, non-electrochemical methods take hours and days to diagnose cholera and require specialist skills to execute and thus are incompatible for fast diagnosis and field screening. For example, the culture method, which is the gold standard for the detection of cholera, involves the isolation of the bacteria from stool samples on selective media followed by biochemical identification and serotyping with monoclonal antibodies.[10] The culture method is disadvantageous as it is time consuming and requires several media/reagents as well as specialist skills to perform. It is a multistep technique, requiring such steps as enrichment with media and incubation at 35−37 °C for 18−24 h. The delay in detecting the infection allows cholera to kill

Received: November 10, 2019
Accepted: February 18, 2020
Published: March 12, 2020

https://dx.doi.org/10.1021/acsomega.9b03820
ACS Omega 2020, 5, 5762−5771

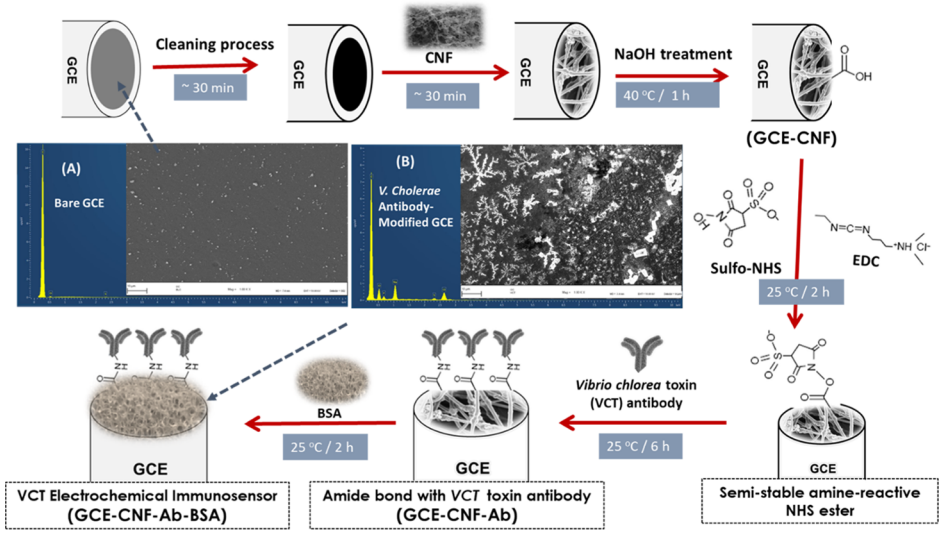

Figure 1. Experimental protocol (and time needed) for the fabrication and sensing mechanism of an electrochemical immunosensor for VCT. The fabrication process takes approximately 12 h. Abbreviations: EDC = 1-ethyl-3-(3-dimethylaminopropyl)carbodiimide hydroxide; sulfo-NHS = *N*-hydroxysulfosuccinimide. Inset (A) shows typical scanning electron micrograph (SEM) and energy dispersive X-ray (EDX) of bare GCE, confirming mostly the C content, while (B) shows the SEM and EDX of *V. cholerae* antibody-modified GCE, showing the presence of C, O, S, F, Na, and Cl, which may be related to the cholera antibody, linking agents, and saline solutions from which the immunosensor was prepared. While the bare GCE is smooth (homogeneous), the modified GCE surface exhibited a highly heterogeneous surface with a dendrite- or lichen-like morphology.

very fast, with death occurring in 12−24 h if untreated.[4] It takes approximately 8 days to confirm the cholera case.[21] PCR combined with culture method results gives enhanced specificity,[22] but it is very costly and time consuming. Most researchers use expensive and/or difficult-to-prepare materials for developing immunosensors.[9−14,17,20−22] In electrochemistry, for example, Palomara et al.[20] used copper(II) complex functionalized via electrocoating of polypyrrole-nitrilotriacetic acid [poly(pyrrole-NTA)] on multi-walled carbon nanotubes (Cu^{2+}/pp-NTA/MWCNTs). Tshikalaha and Arotiba[17] employed the generation-2 poly(propylene imine) (PPI) dendrimer and gold nanoparticles (AuNPs) electro-co-deposited on a glassy carbon electrode (GCE) for the detection of cholera toxin. With the exception of Gupta et al.,[18,19] who reported that the current response increases with the increasing concentration of the cholera toxin, every other report to date on the electrochemical detection of cholera toxin involved the suppression of the current response upon increasing the concentration of the cholera toxin. In all cases, there is a need to develop electrochemical immunosensors that use low-cost carbon materials that are easy to prepare and deploy as an electrode platform that allows for fast, sensitive, and reliable detection of *V. cholerae* toxin (VCT).

Electrochemical techniques offer most advantages for the detection of cholera because they are simple to operate, very sensitive, specific, rapid, and low cost and can be miniaturized for portability and point-of-care diagnosis. In this work, we interrogated the possibility of developing highly sensitive and selective electrochemical immunosensors for *V. cholerae* in water samples using carbon nanofibers (CNFs). This is the first time that CNF has been reported for application as a viable electrode platform for the detection of *V. cholerae*. The choice for CNF is motivated by several reasons. Most importantly, serendipitously, we made a new finding on the use of the "aged" redox probe to improve the sensitivity of detection of *V. cholerae* in real cholera-infested water samples. We believe that this unique observation strongly highlights the importance of considering the nature of the redox probe on the electrochemical sensing conditions, especially when designing impedimetric immunosensors.

2. RESULTS AND DISCUSSION

2.1. Electron-Transfer Dynamics of the Electrodes.

Electrospun CNFs used as the platform for the electrochemical immunosensors for cholera toxin in this work were obtained using the conventional electrospinning technique.[23,24] The fabrication of the electrochemical immunosensor [i.e., GCE modified with CNF, antibody (Ab), and bovin serum albumin (BSA)] adopted the conventional method of covalently linking the antibody onto the electrode platform.[25,26] The immunosensor (GCE−CNF−Ab−BSA) is ready to be used for the sensing of the antigen (Ag), also described as VCT. The various steps involved have been schematically represented in Figure 1 (described in detail in the Experimental Section). To understand the extent to which the immunosensor permits the redox probe to transport the electron, the bare GCE and its modified surfaces (GCE−CNF to GCE−CNF−Ab−BSA) were subjected to cyclic voltammetry (CV) and electrochemical impedance spectroscopy (EIS) experiments in a 0.14 M phosphate-buffered saline (PBS)/AE (pH 7.4) containing a redox probe, 0.1 M $[Fe(CN)_6]^{3-}$/$[Fe(CN)_6]^{4-}$ solution (see the Supporting Information, Figure S2). The choice of a high concentration of the redox probe has been informed mainly by the need to eliminate the diffuse layer effect (Frumkin effect), as clearly articulated in the literature[27−30] (also see the explanation for Figure S2 in the Supporting Information).

From the CV profiles, the electron-transfer properties could be established from the following parameters (summarized in the Supporting Information, Table S1): (i) the ratio of the anodic-to-cathodic peak current heights (I_{pa}/I_{pc}), which should be unity for an ideal reversible process; (ii) the voltammetric current response, which defines the mass transport; and (iii)

https://dx.doi.org/10.1021/acsomega.9b03820
ACS Omega 2020, 5, 5762−5771

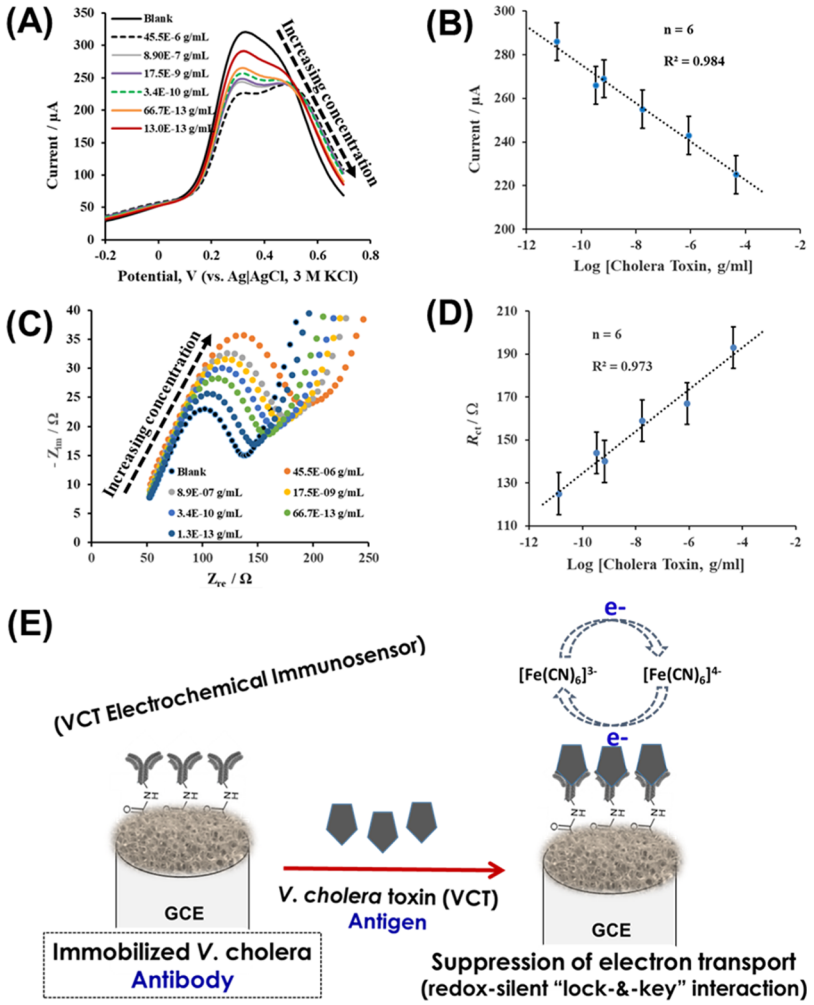

Figure 2. (A) SWV responses of the GCE-modified immunosensor (GCE−CNF−Ab−BSA) at different concentrations of VCT (1.30×10^{-13} to 45.50×10^{-6} g mL^{-1}); (B) SWV-measurement calibration curve for the detection of VCT; (C) Nyquist plots (Z_{im} vs Z_{re}) for the EIS measurements at different VCT concentrations as in (A); (D) EIS-measurement calibration curve for the detection of VCT. All measurements (SWV and EIS) were obtained in 0.14 M PBS/AE (pH 7.4) containing 0.1 M $[Fe(CN)_6]^{3-}/[Fe(CN)_6]^{4-}$; and (E) the mechanism of interaction between the VCT antibody−antigen that leads to the suppression of the electron transport; thus, the increase in impedance as the concentration of the VCT antigen is increased. The broken arrows simply depict poor electron transport.

the peak-to-peak separation potential (ΔE_p), which defines the rate of electron transfer, which is 0.059 V/n for a one-electron reversible reaction (the smaller it is, the faster is the electron transfer, and vice versa). The ΔE_p decreases as follows: GCE (0.230 V) < GCE−CNF (0.256 V) < GCE−CNF−Ab (0.322 V) < GCE−CNF−Ab−BSA (0.620 V), indicating that the GCE−CNF−Ab−BSA gives the strongest resistance to electron transport. The I_{pa}/I_{pc} follows a similar trend, meaning that GCE−CNF−Ab−BSA is the least reversible, while GCE and GCE−CNF are the most reversible. The results indicate that the ET processes between the redox probe and the underlying GCE surface become difficult as the modifying redox-inactive layers are increased. On the other hand, the voltammetric current response decreases as follows (using the anodic peak current, I_{pa}, as example): GCE (1.55 mA) > GCE−CNF (0.95 mA) > GCE−CNF−Ab (0.89 mA) > GCE−CNF−Ab−BSA (~0.3 mA), which defines the level of mass transport (i.e., the rate at which the redox probe solution moves from the bulk electrolyte solution to the electrode surface). The current generated at the surface of the porous electrode is due to two diffusion processes: (i) *semi-infinite planar diffusion* (in this case, the redox probe solution toward the macro-electrode surface) and (ii) *thin-layer diffusion* (i.e., a small volume of the redox probe solution trapped in pockets within the porous structure).[31] Thin-layer diffusion, combined with the semi-infinite diffusion, enhances the overall current response of the electrode. However, if the electrolyte in the pores of the porous electrode film is significantly depleted of the electroactive species on the experiment timescale, then the overall current response will be diminished. Thus, the high current response of the GCE is related to its nonporous surface that encourages semi-infinite diffusion but discourages the trapping of the electrolyte. On the other hand, the porous nature of the other electrodes (CNF, CNF−Ab, and CNF−Ab−BSA) allows for the trapping of the redox probe species longer than the experimental timescale, hence the reduced current response. The slightly higher current response of the CNF−Ab over the CNF is interpreted in terms of the Ab permitting the thin layer diffusion compared to the CNF.

In addition, the surface coverage of the antibody was estimated from the CV evolution of the redox probe (see the Supporting Information). The values of the surface coverage were approximately 2.68×10^{-7} and 2.86×10^{-7} mol cm^{-2} for the GCE−CNF and GCE−CNF−Ab, respectively. These

https://dx.doi.org/10.1021/acsomega.9b03820
ACS Omega 2020, 5, 5762−5771

Table 1. Comparative Electrochemical Detection Parameters of the Recent Literature Using Different Immunosensor Platforms for the Electrochemical Detection of Cholera[a]

sensor platform/technique	LCR (g mL^{-1})	sensitivity	LoD (g mL^{-1})	LoQ (g mL^{-1})	refs
nanoporous ZnO/ITO (DPV)	12.5×10^{-9} to 5.00×10^{-7}	71	16×10^{-11}		18
PANnf/ITO (DPV)	6.25×10^{-9} to 5.00×10^{-7}	90 nA/ng mL/cm^2	22×10^{-11}		19
PPI-AuNP composite/GCE (SWV, EIS)	10^{-7} to 10^{-12}		7.2×10^{-13} (SWV), 4.2×10^{-13} g (EIS)		17
Cu^{2+}/pp-NTA/MWCNTs/GCE (EIS)	10^{-13} to 10^{-5}	24.7 Ω per order of magnitude	$\sim 10^{-13}$		20
CNF/GCE, SWV (EIS)	1.3×10^{-13} to 4.56×10^{-5}	9.775 Ω per order of magnitude	1.25×10^{-13}	1.31×10^{-13}	this work

[a]ITO: indium tin oxide; PANnf = polyacrylonitrile nanofiber; PPI-AuNP/GCE = generation 2 poly(propylene imine) dendrimer (PPI) and gold nanoparticles (AuNPs) electro-co-deposited on a GCE; Cu^{2+}/pp-NTA/MWCNTs = copper(II) complex functionalized via electrocoating of polypyrrole-nitrilotriacetic acid [poly(pyrrole-NTA)] on MWCNTs.

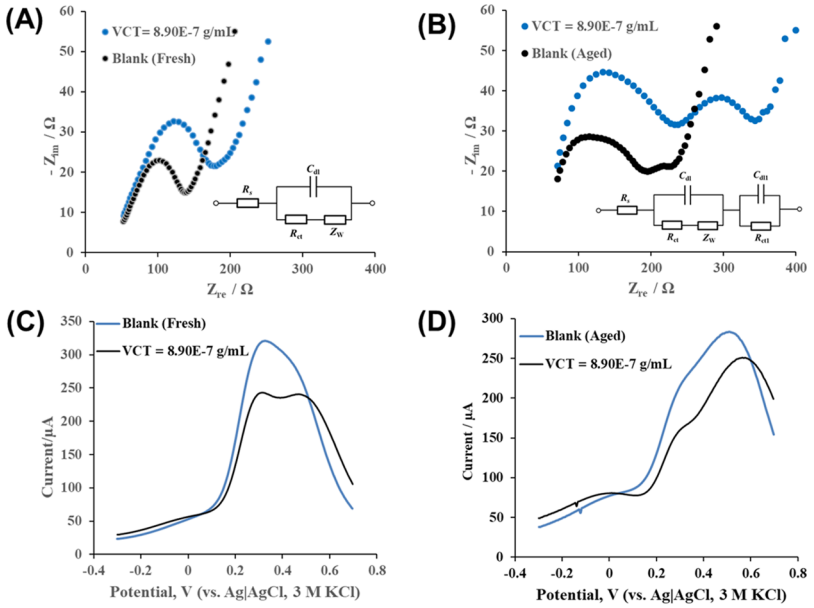

Figure 3. Typical (A,B) EIS and (C,D) SWV measurements at the GCE-modified immunosensor (GCE−CNF−Ab−BSA) for the detection of VCT (8.9×10^{-7} g mL^{-1}) using (A,C) freshly prepared redox probe (0.1 M $[Fe(CN)_6]^{3-}/[Fe(CN)_6]^{4-}$ in 0.14 M PBS/AE, pH 7.4) (used with 24 h) and (B,D) the same redox probe after storing for 30 days at normal room temperature.

results demonstrate that the amount of the antibody on the CNF is extremely small, ca. 1.8×10^{-8} mol cm^{-2}.

2.2. Electrochemical Detection of Cholera Toxins: Calibration Curve. The electrochemical detection of VCT at the GCE−CNF−Ab−BSA immunoelectrode was carried out at different concentrations of VCT (45.5 μg/mL to 0.13 pg/mL, obtained via serial dilutions) with square wave voltammetry (SWV) (Figure 2A,B) and EIS (Figure 2C,D) in 0.1 M $[Fe(CN)_6]^{3-}/[Fe(CN)_6]^{4-}$/0.14 M PBS/AE solution (pH 7.4) at its equilibrium potential ($E_{1/2}$ = 0.26 V vs Ag/AgCl, 3 M KCl). Prior to electrochemical testing, 10 μL of VCT was drop-cast onto the surface of the immunoelectrode and incubated for 20 min at 25 °C. In contrast to the literature,[18,19] we observed that the SWV current response decreased with the increasing VCT concentration (Figure 2A,B). This decrease in the current response is indicative of the formation of the antibody−antigen complex of the *V. cholerae* toxin on the immunoelectrode surface, which is non-conducting (i.e., insulating or redox inactive). Moreover, the resolution of the SWV is so poor that it shows weak double peaks for each of the samples; the reason for this behavior is unknown at this moment but may be related to possible disruption/re-arrangement of the "lock-and-key" bond of the antibody−antigen complex during the voltammetric process. Efforts to extend the potential window from −0.2 to 1.4 V (vs Ag|AgCl, 3 M KCl) did not yield any positive result.

The corresponding behavior was observed with the EIS (Figure 2C,D), where the combined resistances in series (i.e., $R_{ts} = R_{ct1} + R_{ct2}$) increased with increasing VCT concentrations. Figure 2E is a schematic representation of the "lock-and-key" antibody−antigen interaction mechanism. Each point on the SWV- and EIS-based calibration graphs represents the average value obtained from replicate measurements (n = 6). The limit of detection (LoD) is defined as the lowest concentration of VCT that produces a reading of 3s (where s is the standard deviation of the blank signal) above the blank signal, under the same experimental conditions. The limit of quantification/determination (LoQ = 10s) is defined as the concentration of the VCT sample that produces a signal that cannot be confused with that of the blank solution and that could be quantified.[32,33] Both SWV and EIS techniques gave a good linear concentration range (LCR) for VCT (1.3×10^{-13}

https://dx.doi.org/10.1021/acsomega.9b03820
ACS Omega 2020, 5, 5762−5771

to 4.56×10^{-5} g mL^{-1}, $R^2 > 0.99$). At higher VCT concentrations (>46×10^{-6} g mL^{-1}), the current or charge transfer resistance measured by the immunosensor reached saturation, accompanied by poor performance of the sensor due to overload of the biomaterials on the surface. Both SWV and EIS techniques gave high sensitivity toward VCT detection: −8.813 μA/log[VCT] (g mL^{-1}) for SWV and 9.775 Ω/log[VCT (g mL^{-1})] for EIS. The LoD and LoQ were estimated as 1.25×10^{-13} and 1.31×10^{-13} g mL^{-1}, respectively. Repeat concentration studies were conducted using same samples prepared for Figure 2 after about 2 months (see the Supporting Information, Figure S3). Interestingly, albeit there was a slight change in the shape of the response curves (especially the EIS) compared to the fresh sample analysis (Figure 2), there was no significant change in the concentration curve graphs. Table 1 compares the electrochemical detection parameters using different platforms for cholera immunosensors with some recent literature. Clearly, our platform (CNF) not only is simple to fabricate, but also proves to be efficient for enhanced electrochemical detection compared to the literature (in terms of wider LCR and low LoD and LoQ).

2.3. Aging Effect of the Redox Probe on the Capacitive Detection Protocols. Redox probe (notably $[Fe(CN)_6]^{3-}/[Fe(CN)_6]^{4-}$) commonly serves as the critical element of the EIS-based immunosensing.[34−39] In other words, the stability or chemistry of the redox probe has a direct relationship to the sensitivity of the immunosensor. Out of curiosity, we decided to test the immunosensor in freshly prepared (used within 24 h after preparation) and aged solution (after 30 days of preparation, stored at room temperature) of $[Fe(CN)_6]^{3-}/[Fe(CN)_6]^{4-}$, and to our surprise, we observed different EIS and SWV data for blank and VCT analytes (Figure 3). There are some important findings here, especially for EIS: first, unlike the fresh solution of the redox probe (Figure 3A) that was fitted with a simple Randles circuit ($\sim R_s(C_{dl}[R_{ct}Z_w])\sim$), the aged redox probe (Figure 3B) solution was fitted with the Randles−Voigt circuit with one *RC* element ($\sim R_s(C_{dl}[R_{ct}Z_w])(R_{ct1}C_{dl1})\sim$). Second, from the fitted parameters (Table 1), there is a slight increase in the electrolyte resistance (R_s) value from ∼66 Ω (for the fresh) to ∼82 Ω (for the aged), indicative of some changes in the chemistry of the original solution. Third, there is an increased sensitivity of VCT detection (i.e., high value of the total charge resistance) upon aging of the redox probe. Fourth, and most importantly, the last semicircle (R_{ct1}) is more pronounced for the VCT analyte and can possibly serve as a unique *signature polarization resistance* (hereinafter abbreviated as R_{spr}) for the interaction of VCT with the immunosensor. This was tested and found to be true (see the next section on a real water sample analysis). The enhanced sensitivity of the VCT detection arising from the aging of the redox probe may be described as Redox Probe Ageing-Induced Sensitivity Enhancement (abbreviated herein as "Redox-PrAISE"). Similar experiments were carried out for SWV (Figure 3C,D), with the aged solution showing broader and lower peak current responses at a higher potential (∼0.5 V vs Ag/AgCl, 3 M KCl) compared to the fresh redox solution (∼0.3 V vs Ag/AgCl, 3 M KCl), confirming increased electrolyte resistivity and poorer charge transport properties (excellently corroborating the EIS data of Figure 3A,B, as also shown in Table 2). Thus, subsequent measurements were focused on the more sensitive EIS-based Redox-PrAISE for VCT detection.

Table 2. Typical EIS Data Obtained for the Immunosensor (GCE−CNF−Ab−BSA) Fresh (within 24 h) and Aged (30 days) Solutions of the Redox Probe (i.e., 0.1 M $K_4Fe(CN)_6$/$K_3Fe(CN)_6$ in 0.14 M PBS/AE) at 0.26 V (vs AglAgCl 3 M KCl) in the Absence (Blank Solution) and Presence of VCT (VCT = 8.90×10^{-7} g mL^{-1})[a]

	electrochemical impedance spectral parameter					
sample	R_s/Ω	$C_{dl}/\mu F$	R_{ct}/Ω	$C_{dl}/\mu F$	R_{ct1}/Ω	$Z_w/\Omega\ s^{-1/2}$
Fresh Probe Solution						
blank solution (fresh probe)	66.4	33.30	70.90			0.026
VCT sample (fresh probe)	66.1	34.20	103.50			0.024
Aged Probe Solution						
blank solution (aged probe)	81.8	3.25	77.10	289.60	57.50	0.035
VCT sample (aged probe)	82.0	2.84	125.80	506.10	102.80	0.035

[a]All values were obtained from the fitted impedance spectra ($n = 3$). Average percentage errors in fitting ≤10%.

The reason for the aging of the $[Fe(CN)_6]^{3-}/[Fe(CN)_6]^{4-}$ solution and its implications on the sensitivity of the immunosensor is not fully understood at the moment and requires a detailed future investigation. However, from a body of literature, it has been known that ferricyanide/ferrocyanide can decompose due to the cleavage of CN under UV irradiation[40] and electron irradiation[41−43] and, recently, by intense synchrotron radiation via in situ X-ray absorption spectroscopy,[44] which led to the precipitation of the passivating ferric (hydr)oxide species that inhibited the redox process of the ferri-/ferrocyanide. Thus, it is highly possible that our finding in this work is due to the decomposition of the $[Fe(CN)_6]^{3-}/[Fe(CN)_6]^{4-}$ solution occurring at a slower rate at normal room temperature. This is an important preliminary observation for the redox probe-based electrochemical detection. Since this has never been reported in the literature, there is a need for further interrogation in the future.

2.4. Regeneration of the Immunosensor Surface. The regeneration study of the immunoelectrode surface was carried out in three steps: First, the immunosensor was immersed in PBS/AE containing antigen (VCT) for 20 min. Second, it was washed in a PBS/AE buffer solution and distilled de-ionized water and dried in nitrogen gas. Third, it was used for the detection of VCT (8.90×10^{-7} g mL^{-1}). Finally, the immunosensor was dipped into a glycine HCl buffer (pH 2.8) for 5 min (to remove the bound antigen cells). These steps were repeated 4−5 times to determine the percentage changes in the signal (if any). A typical SWV regeneration study is exemplified in Figure S4. SWV and the bar chart of the current response versus VCT concentration after different regeneration (Supporting Information, Figure S4) clearly show, within limits of errors, no significant change in current response. The result shows that the immunosensor surface can be regenerated and reused a few times for the detection of VCT. The chemistry behind the regeneration with glycine is known.[45] Glycine is an amino acid that is zwitterionic. It is able to bind to the surface of the bioreceptor (immunosensor) as well as the bioanalyte due to the thermodynamic feasibility of such a binding process. Thus, when the bioreceptor is exposed

https://dx.doi.org/10.1021/acsomega.9b03820
ACS Omega 2020, 5, 5762−5771

to the regeneration buffer containing glycine, it is partially protected from the damage arising from the change in the pH environment.

2.5. Selectivity/Interference Studies. Selectivity/interference studies were carried out in the presence of the interferents in physiological fluids or environment, with 0.5 mM stock solutions of ascorbic acid (AA), citric acid (CA), and uric acid (UA), respectively. During the measurements, the same concentration (0.5 mM) of each of the interferents (AA, CA, and UA) was mixed with a fixed VCT concentration (8.90×10^{-7} g mL^{-1}), and the electrochemical response after 20 min incubation time was observed and recorded. Typical SWV measurements (Supporting Information, Figure S5) showed no detectable difference in the current responses of the VCT sample in the absence and presence of the physiological interfering molecules. This is not totally surprising considering that antibody−antigen interactions are known for their unique specificity/selectivity.

2.6. Determination of VCT in Water Samples. Considering the higher sensitivity of the proposed EIS-based Redox-PrAISE method over the SWV counterpart, it was used for the analysis of different water samples obtained from local water bodies that were suspected to be cholera infested. However, prior to the Redox-PrAISE experiment, the water samples were tested for being contaminated with *V. cholerae* by using the culture method.[46] The suspected water was collected (Figure 4A), 2 mL of the water sample was inoculated in

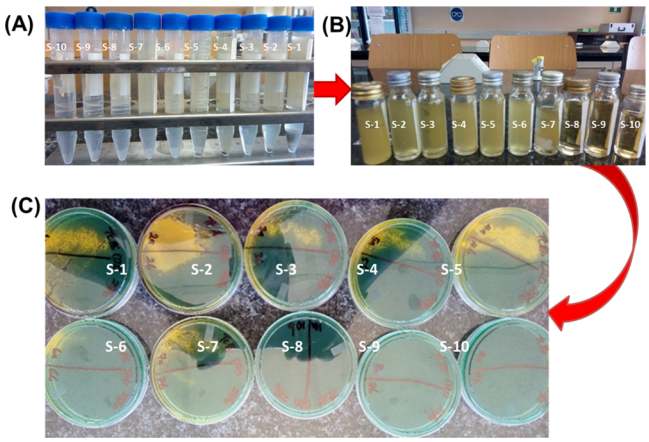

Figure 4. Steps for the culture method of detecting *V. cholera*: suspected water was collected (A), 2 mL of the water sample was inoculated in APW and incubated/cultured for 12 h at 37 °C in ambient air (B); then, it was sub-cultured in TCBS agar as the selective medium for 24 h at 37 °C in ambient air (C). The suspected cholera-infected samples are labeled S1−S8, while sample S9 (bottled water) and S10 (alcohol−water mixture: 70% alcohol, 30% tap water) serve as controls. All the photos were taken during the course of this study by Ozoemena.

alkaline peptone water (APW) and incubated/cultured for 12 h at 37 °C in ambient air (Figure 4B), and then, it was sub-cultured in thiosulfate citrate bile salt sucrose (TCBS agar) as the selective medium for 24 h at 37 °C in ambient air (Figure 4C). Note that APW is the preferred enrichment broth for the isolation of *V. cholera* present in any sample (be it clinical, food, or water). APW is characterized by its light-yellow-colored clear solution appearance. The presence of *V. cholerae* growing on TCBS agar plates is indicated by a yellow coloration. In this work, the suspected cholera-infested water samples are labeled S1−S7, S8 (tap water), S9 (bottled water), and S10 (alcohol−water mixture: 70% alcohol, 30% tap water). The contamination of samples with *V. cholera* is easily established by a turbid or cloudy growth with APW. As clearly evident in Figure 4B, the turbidity level decreases as S1 > S2 > S3 > S4 > S5 > S6 > S7 ≫ S8 ≈ S9 ≈ S10. The trend is essentially the same for the TCBS agar plates (Figure 4C), suggesting that samples S8−S10 showed no detectable presence of *V. cholera*.

Next, the Redox-PrAISE experiment was conducted as described before, focusing on the signature polarization resistance (R_{spr}), as depicted in Figure 5A,B. It is interesting to observe that the VCT concentrations in the samples are more clearly defined in the *RC* elements of the low-frequency region (shown as oval, i.e., R_{spr}) than in the high-frequency region, confirming the choice for the application of R_{spr} as the signature charge-transfer resistance for cholera toxin infection in water samples in this work.

The change in the total charge-transfer resistance ($\Delta R_{ct}/\Omega$) for each water sample, control, or standard solution was calculated in accordance with the literature[34,35]

$$\Delta R_{ct} = R_{Ag\text{-}VCT} - R_{Ag} \quad (1)$$

where R_{Ag} is the immunosensor resistance of the blank solution, while $R_{Ag\text{-}VCT}$ is the value of the immunosensor resistance after incubation with the water samples and control solutions. Figure 5C represents the bar chart of ΔR_{ct} against the various water samples (S1−S10, including the standard VCT sample (8.90×10^{-7} g mL^{-1}) and blank PBS/AE solution) using the full polarization resistance and the signature resistance (R_{spr}) alone. Samples S9 and S10 showed no presence of cholera in excellent agreement with the culture method. However, note that EIS showed some presence of cholera infection in S8, seemingly lower than the detection limit of the culture method, which may explain the high sensitivity of the EIS method. In fact, high sensitivity is a key signature of the EIS method, and this is well reported in the literature that even the smallest amounts of analytes, such as antibodies or antibody-related substances,[36,37] can provoke measurable changes with EIS, allowing high sensitivities[38] even to the femtomolar levels.[39]

3. CONCLUSIONS

The application of electrospun CNFs as viable electrode platforms for the development of simple and highly sensitive immunosensors for VCT has been described. The immunosensor was easily fabricated by adopting the carbodiimide chemistry that allows for a strong amide bond formation between the amino groups of the antibody and the carboxylic groups of the base electrode platform. The sensing signal, which is the suppression of electric current, can easily be followed by the SWV or EIS technique, the latter being more preferable as it is more sensitive than the former. One of the findings is the ability of the aged redox probe (ferri-/ferrocyanide solution) to enhance the sensitivity of the immunosensor for the detection of VCT. This observation, termed the "Redox Probe Ageing-Induced Sensitivity Enhancement" ("Redox-PrAISE"), highlights the importance of the nature of the redox probe on the electrochemical sensing conditions when designing impedimetric immunosensors. Further research is necessary to investigate and apply this finding to other biological analytes. In general, the

https://dx.doi.org/10.1021/acsomega.9b03820
ACS Omega 2020, 5, 5762−5771

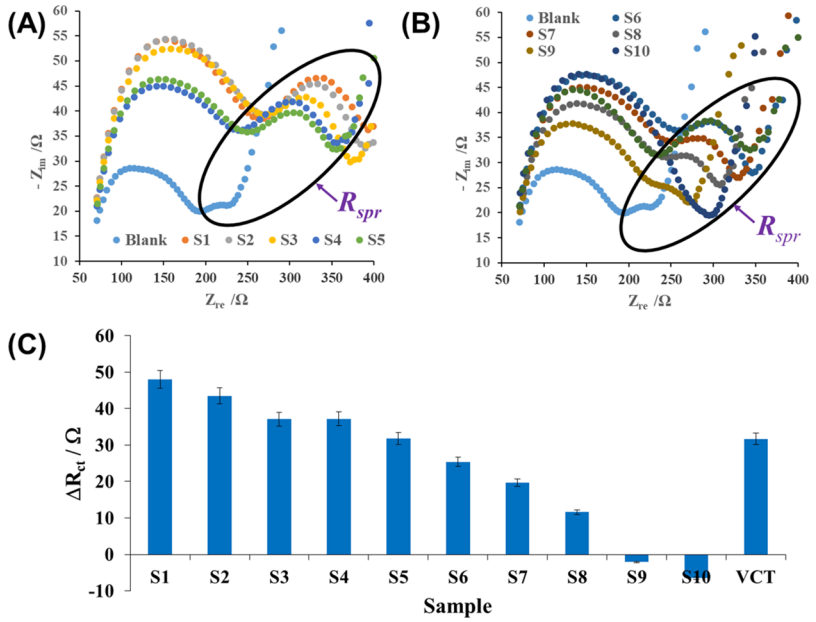

Figure 5. (A,B) EIS measurements at the GCE-modified immunosensor (GCE−CNF−Ab−BSA) for the detection of VCT in real water samples using an aged redox probe (0.1 M $[Fe(CN)_6]^{3-}/[Fe(CN)_6]^{4-}$ prepared with 0.14 M PBS/AE, pH 7.4) at normal room temperature. The same water samples used for the culture analysis in Figure 4 are used here: suspected cholera-infected samples are labeled S1−S8, while sample S9 (bottled water) and S10 (alcohol−water mixture: 70% alcohol, 30% tap water) serve as controls. Note that (A,B) are separated for clarity. (C) Represents the bar chart of the $\Delta R_{ct}/\Omega$ vs water samples.

immunosensor showed an excellent performance in terms of sensitivity, selectivity, and regenerability: very low limits of detection (ca. 1.2×10^{-13} g mL^{-1}) and quantification (ca. 1.3×10^{-13} g mL^{-1}) at a wide LCR of 8 orders of magnitude (10^{-13} to 10^{-5} g mL^{-1}). When subjected to a real sample application using cholera-infested water samples, the immunosensors exhibited comparable or even better results than the gold standard clinical culture method. This opens a new window of opportunities for the optimization and potential application in the point-of-care diagnosis of *V. cholerae* infection, especially in resource-limited countries plagued by the constant occurrence of the cholera epidemic.

4. EXPERIMENTAL SECTION

4.1. Materials and Reagents. The following chemicals/specialty reagents were obtained from Sigma-Aldrich: polyacrylonitrile (PAN) polymer; *N*,*N*-dimethylformamide (DMF); glycine (PharmaGrade, Ajinomoto, EP, product no. G5417); anti-cholera toxin antibody (Ab) produced in rabbit (delipidized, whole antiserum, cat. no. C3062); VCT B subunit (from *V. cholerae* cat. no. C9903, 95% sodium dodecyl sulfate-polyacrylamide gel electrophoresis, lyophilized powder), which is the antigen (Ag); (1-ethyl-3-(3-dimethylaminopropyl)-carbodiimide)hydrochloride (EDC); *N*-hydroxysulfosuccinimide (sulfo-NHS); Nafion perfluorinated resin solution (5 wt % in lower aliphatic alcohols and water; contains 15−20% water); and BSA (heat shock fraction, pH 7, ≥98%). TCBS was obtained from Sigma-Aldrich. Ultra-pure water of resistivity 18.2 M Ω cm was obtained from a Milli-Q Water System (Millipore Corp. Bedford, MA, USA) and used throughout for the preparation of solutions. All other reagents used in this work were of pure analytical grade and used as received from the suppliers without further purification. PBS containing sodium azide (0.025%, m/v) and 1 mM EDTA (0.14 M PBS/AE, pH 7.4) was prepared following our previous methods:[35,37] briefly, sodium azide (0.025%, m/v), 0.2922 g (1 mmol) EDTA, 0.2 g (1.5 mmol) KH_2PO_4, 1.05 g (7.4 mmol) Na_2HPO_4, 8.0 g (0.14 mol) NaCl, and 0.2 g (2.7 mmol) KCl were dissolved and made up to 1 L mark of the volumetric flask with ultra-pure water. The role of the azide is to serves as a preservative, while EDTA is for disengaging cells that may be attached to the containing vessels or clumped together. The 0.1 M $K_4Fe(CN)_6/K_3Fe(CN)_6$ (1:1) mixture was prepared in 0.14 M PBS/AE, pH 7.4; typically, 1.6462 g (5 mmol) $K_3Fe(CN)_6$ and 2.1121 g (5 mmol) $K_4Fe(CN)_6$ were dissolved in 50 mL PBS/AE.

4.2. Preparation of Electrospun Carbon Nanofibres. Electrospun CNFs were obtained using the conventional electrospinning technique.[23,24] In this work, electrospinning works were carried out using the KD Scientific model syringe pump (KD Scientific Inc., USA). Briefly, 2 g of PAN polymer was weighed, dispersed in 15 mL of 100% w/w DMF, and ultrasonicated for 20 min at room temperature to allow for a thorough dissolution. The resulting polymer solution was filled in the syringe to perform the conventional electrospinning process at 10 kV power supply at room temperature. The distance between the syringe point and the collector plate was maintained at about 15 cm, while the flow rate of the polymer solution was 0.6 mL/h. On completion, the fiber materials were removed from the aluminum plate collector, then soaked in distilled deionized water overnight (∼12 h) to extract or wash off the solvent (DMF), and dried in an oven at 60 °C for 2 h to obtain a white fluffy PAN fiber. Subsequently, the white PAN fiber material was stabilized by heating at 300 °C for 3 h and finally carbonized at 800 °C in an argon atmosphere for 7 h to obtain the CNFs. The typical scanning electron microscopic (SEM) image (obtained from the Zeiss FIB-SEM at the NMISA, Pretoria) of the CNFs (see the Supporting Information, Figure S1) comprises a mixture of

https://dx.doi.org/10.1021/acsomega.9b03820
ACS Omega 2020, 5, 5762−5771

agglomerated fibers, mostly of the nano-sized dimensions (40−200 nm), with few fibers reaching the micrometric dimensions.

4.3. Electrochemical Procedures. Electrochemical experiments were carried out using an Autolab Potentiostat PGSTAT 100 (Eco Chemie, Utrecht, the Netherlands) powered by the 4.9 version of GPES and FRA softwares. The working electrode was glassy carbon disk electrode [GCE, Bioanalytical Systems (BAS), diameter = 3.0 mm] modified with the CNF. A Pt rod was used as the counter electrode, while Ag/AgCl (3 M KCl) was used as the reference electrode. Both CV and SWV were used. The following SWV parameters were used throughout the work: frequency of 10 Hz, step potential of 5 mV, and amplitude of 20 mV. EIS experiments were conducted using an Autolab frequency response analyzer (FRA) software between 100 kHz and 10 mHz with the amplitude (rms value) of the ac signal of 10 mV in a solution of 0.1 M $K_4Fe(CN)_6/K_3Fe(CN)_6$ (1:1) mixture in 0.14 M PBS/AE (pH 7.4) and at the equilibrium potential ($E_{1/2}$) of the redox probe, $[Fe(CN)_6]^{3-}/[Fe(CN)_6]^{4-}$ (~0.126 V vs AgI AgCl, 3 M KCl). The raw EIS experimental data were fitted with the FRA software using the appropriate electrical equivalent circuit models. All solutions were de-aerated by bubbling pure nitrogen (Afrox, South Africa) prior to each electrochemical experiment. All experiments were performed at room temperature.

4.4. Fabrication of the Electrochemical Immunosensor. The bare GCE was first thoroughly cleaned using slurries of aluminum oxide nano-powder (50 nm, Sigma-Aldrich) on a Buehler felt pad, followed by ultrasonic cleaning in ethanol and acetone to remove residual alumina nano-powder and obtain a mirror-finish surface. The method of drop-drying was used for the modification of GCE with the samples: 2 mg of the CNF was dispersed in 2 mL DMF containing 20 μL 5% Nafion and ultra-sonicated for about 30 min. Thereafter, 10 μL of the mixture was drop-cast onto the GCE surface and slowly dried in oven at about 40 °C (abbreviated here as GCE−CNF). To remove carboxylated carbonaceous fragments from the carboxyl functioning group (−COOH) on the carbon surfaces, each of the GCE-modified surface was immersed in a 2 M NaOH solution for 1 h at 40 °C and allowed to cool to room temperature. The EDC/sulfo-NHS mixture (10 μL; 1:1 v/v ratio) was dissolved in 2 mL PBS/AE (pH = 7.4) dropwise unto the surface of the electrode. EDC serves as the coupling or cross-linking agent that activates the −COOH (i.e., generating an *o*-acylisourea species, which is unstable in an aqueous solution), while NHS assists in stabilizing this intermediate by converting it to an amine-reactive ester (which is a more stable species) for the coupling of the incoming $-NH_2$ group of the *V. cholerae* antibody (Ab) to form a strong amide (−NHCO−) bond.

Prior to the immobilization of the Ab on the functionalized carbon surfaces, the as-received anticholera toxin (Ab) was defrosted by removing from the refrigerator and allowed to stand for about 30 min at room temperature. 25 μL of the as-received Ab was diluted 5 times with PBS (1:5) and sonicated for a few minutes. 10 μL (0.01 mg/mL in PBS/AE, pH 7.4, 10 mM) of the solution was added dropwise on the surface of the functionalized GCE-modified surfaces and incubated under humid condition overnight at room temperature. This was followed by washing the electrode [swirling gently or rinsing using a copious amount of PBS/AE (i.e., pH 7.4, 10 mM)] to remove the unbound antibody (the modified electrode is abbreviated herein as GCE−CNF−Ab). Then, 10 μL of BSA (0.01 mg/mL) was added to the surface of the electrode and incubated for 4 h (abbreviated as "GCE−CNF−Ab−BSA"; note that BSA was used to block nonspecific sites on the porous surface of the electrode). Finally, the electrode was rinsed in PBS/AE and doubly distilled and deionized water, dried using nitrogen stream, used immediately, or stored in a refrigerator at 4 °C until needed for electrochemical experiments. The BSA-modified electrode was used for the electrochemical detection of the as-received cholera antigen/toxin (VCT) at different concentrations/dilutions (notably from 45.5 μg/mL to 130 ng/mL), using SWV and EIS. Different concentrations of VCT were first prepared via serial dilutions from the stock solution and stored at 4 °C when not in use.

■ ASSOCIATED CONTENT

Supporting Information

The Supporting Information is available free of charge at https://pubs.acs.org/doi/10.1021/acsomega.9b03820.

Typical SEM image of the electrospun CNFs; comparison of the cyclic voltammograms of the GCE modified with CNF, CNF−Ab, and CNF−Ab−BSA in 0.1 M $K_4Fe(CN)_6/K_3Fe(CN)_6$ in PBS/AE at 0.26 V (vs AglAgCl, 3 M KCl) at 50 mV/s; repeat concentration studies conducted after 2 months using same samples prepared for Figure 2; typical SWV response and the corresponding bar chart of current response at a constant VCT concentration (8.50×10^{-7} g mL^{-1}); typical SWV response and the corresponding bar chart of current response at a constant VCT concentration (8.90×10^{-7} g mL^{-1}) upon different regeneration; comparing the CV data obtained for the GCE modified with CNF, CNF−Ab, and CNF−Ab−BSA in a redox probe (i.e., 0.1 M $K_4Fe(CN)_6/K_3Fe(CN)_6$ in PBS/AE) at 0.26 V (vs AglAgCl, 3 M KCl) (PDF)

■ AUTHOR INFORMATION

Corresponding Authors

Jerry L. Shai − *Department of Biomedical Sciences, Faculty of Science, Tshwane University of Technology, Pretoria 0001, South Africa*; Phone: +27 123826342; Email: ShaiLJ@tut.ac.za

Kenneth I. Ozoemena − *Department of Chemistry, University of Pretoria, Pretoria 0002, South Africa; Molecualr Sciences Institute, School of Chemistry, University of the Witwatersrand, Johannesburg 2050, South Africa*; orcid.org/0000-0001-7107-7003; Phone: +27 11 717 6730; Email: Kenneth.ozoemena@wits.ac.za

Authors

Okoroike C. Ozoemena − *Department of Biomedical Sciences, Faculty of Science, Tshwane University of Technology, Pretoria 0001, South Africa; Department of Chemistry, University of Pretoria, Pretoria 0002, South Africa*

Tobile Maphumulo − *Molecualr Sciences Institute, School of Chemistry, University of the Witwatersrand, Johannesburg 2050, South Africa*

Complete contact information is available at: https://pubs.acs.org/10.1021/acsomega.9b03820

Notes

The authors declare no competing financial interest.

https://dx.doi.org/10.1021/acsomega.9b03820
ACS Omega 2020, 5, 5762−5771

[‖]OC Ozoemena was a visiting student to the University of Pretoria, where he conducted the electrochemistry experiments.

■ ACKNOWLEDGMENTS

The financial assistance of the National Research Foundation (NRF) toward this research is hereby acknowledged. Opinions expressed and conclusions arrived at, are those of the authors and are not necessarily to be attributed to the NRF. O.C.O. is grateful to the Department of Science and Innovation (DSI)-NRF for the MTech degree in "DSI-NRF Innovation and Priority Research Areas scholarship".

■ REFERENCES

(1) Harris, J. B.; LaRocque, R. C.; Qadri, F.; Ryan, E. T.; Calderwood, S. B. Cholera. *Lancet* **2012**, *379*, 2466−2476.
(2) Morris, J. G.; Acheson, D. Cholera and other types of vibriosis: A story of human pandemics and oysters on the half shell. *Clin. Infect. Dis.* **2003**, *37*, 272−280.
(3) Weil, A. A.; Khan, A. I.; Chowdhury, F.; Larocque, R. C.; Faruque, A. S. G.; Ryan, E. T.; Calderwood, S. B.; Qadri, F.; Harris, J. B. Clinical Outcomes in Household Contacts of Patients with Cholera in Bangladesh. *Clin. Infect. Dis.* **2009**, *49*, 1473−1479.
(4) Sack, D. A.; Sack, R. B.; Nair, G. B.; Siddique, A. Cholera. *Lancet* **2004**, *363*, 223−233.
(5) Gubala, A. J. Multiplex real-time PCR detection of Vibrio cholerae. *J. Microbiol. Methods* **2006**, *65*, 278−293.
(6) WHO. *Cholera Fact Sheet No. 107*: Geneva, February 2014.
(7) Ali, M.; Lopez, A. L.; Ae You, Y.; Eun Kim, Y.; Sah, B.; Maskery, B.; Clemens, J. The global burden of cholera. *Bull. W. H. O.* **2012**, *90*, 209−218.
(8) Keddy, K. H.; Sooka, A.; Parsons, M. B.; Njanpop-Lafourcade, B. M.; Fitchet, K.; Smith, A. M. Diagnosis of Vibrio cholerae O1 Infection in Africa. *J. Infect. Dis.* **2013**, *208*, S23−S31.
(9) Cecchini, F.; Fajs, L.; Cosnier, S.; Marks, R. S. Vibrio cholerae detection: Traditional assays, novel diagnostic techniques and biosensors. *Trends Anal. Chem.* **2016**, *79*, 199−209.
(10) Alam, M.; Hasan, N. A.; Sultana, M.; Nair, G. B.; Sadique, A.; Faruque, A. S. G.; Endtz, H. P.; Sack, R. B.; Huq, A.; Colwell, R. R.; Izumiya, H.; Morita, M.; Watanabe, H.; Cravioto, A. Diagnostic limitations to accurate diagnosis of cholera. *J. Clin. Microbiol.* **2010**, *48*, 3918.
(11) Ramamurthy, T.; Bhattacharya, S. K.; Uesaka, Y.; Horigome, K.; Paul, M.; Sen, D.; Pal, S. C.; Takeda, T.; Takeda, Y.; Nair, G. B. Evaluation of the bead enzyme-linked immunosorbent assay for detection of cholera toxin directly from stool specimens. *J. Clin. Microbiol.* **1992**, *30*, 1783.
(12) Harris, C. C.; Yolken, R. H.; Krokan, H.; Hsu, I. C. Ultrasensitive enzymatic radioimmunoassay: application to detection of cholera toxin and rotavirus. *Proc. Natl. Acad. Sci. U.S.A.* **1979**, *76*, 5336.
(13) Almeida, R. J.; Hickman-Brenner, F. W.; Sowers, E. G.; Puhr, N. D.; Farmer, J. J.; Wachsmuth, I. K. Comparison of a latex agglutination assay and an enzyme-linked immunosorbent assay for detecting cholera toxin. *J. Clin. Microbiol.* **1990**, *28*, 128.
(14) Koch, W. H.; Payne, W. L.; Wentz, B. A.; Cebula, T. A. Rapid polymerase chain reaction method for detection of Vibrio cholerae in foods. *Appl. Environ. Microbiol.* **1993**, *59*, 556−560.
(15) Alfonta, L.; Willner, I.; Throckmorton, D. J.; Singh, A. K. Electrochemical and quartz crystal microbalance detection of the cholera toxin employing horseradish peroxidase and GM1-functionalized liposomes. *Anal. Chem.* **2001**, *73*, 5287−5295.
(16) Viswanathan, S.; Wu, L.-c.; Huang, M.-R.; Ho, J.-a. A. Electrochemical immunosensor for cholera toxin using liposomes and poly (3, 4-ethylenedioxythiophene)-coated carbon nanotubes. *Anal. Chem.* **2006**, *78*, 1115−1121.
(17) Tshikalaha, P.; Arotiba, O. A. Dendrimer Supported Electrochemical Immunosensor for the Detection of Cholera Toxin in Water. *Int. J. Electrochem. Sci.* **2015**, *10*, 10083−10092.
(18) Gupta, P. K.; Khan, Z. H.; Solanki, P. R. One-Step Electrodeposited Porous ZnO Thin Film Based Immunosensor for Detection of Vibrio cholerae Toxin. *J. Electrochem. Soc.* **2016**, *163*, B309−B318.
(19) Gupta, P. K.; Gupta, A.; Dhakate, S. R.; Khan, Z. H.; Solanki, P. R. Functionalized polyacrylonitrile-nanofiber based immunosensor or Vibrio cholerae detection. *J. Appl. Polym. Sci.* **2016**, *133*, 44170.
(20) Palomar, Q.; Gondran, C.; Holzinger, M.; Marks, R.; Cosnier, S. Controlled carbon nanotube layers for impedimetric immunosensors: High performance label free detection and quantification of anti-cholera toxin antibody. *Biosens. Bioelectron.* **2017**, *97*, 177−183.
(21) Nelson, E. J.; Harris, J. B.; Glenn Morris, J., Jr.; Calderwood, S. B.; Camilli, A. Cholera transmission: the host, pathogen and bacteriophage dynamic. *Nat. Rev. Microbiol.* **2009**, *7*, 693−702.
(22) Page, A.-L.; Alberti, K. P.; Mondonge, V.; Rauzier, J.; Quilici, M.-L.; Guerin, P. J. Evaluation of a rapid test for the diagnosis of cholera in the absence of a gold standard. *PLoS One* **2012**, *7*, No. e37360.
(23) Xue, J.; Xie, J.; Liu, W.; Xia, Y. Electrospun nanofibers: new concepts, materials, and applications. *Acc. Chem. Res.* **2017**, *50*, 1976−1987.
(24) Liu, J.; Weng, W.; Xie, H.; Luo, G.; Li, G.; Sun, W.; Ruan, C.; Wang, X. Myoglobin-and Hydroxyapatite-Doped Carbon Nanofiber-Modified Electrodes for Electrochemistry and Electrocatalysis. *ACS Omega* **2019**, *4*, 15653−15659.
(25) Nakajima, N.; Ikada, Y. Mechanism of amide formation by carbodiimide for bioconjugation in aqueous media. *Bioconjugate Chem.* **1995**, *6*, 123−130.
(26) Gao, Y.; Kyratzis, I. Covalent immobilization of proteins on carbon nanotubes using the cross-linker 1-ethyl-3-(3-dimethylaminopropyl) carbodiimide—a critical assessment. *Bioconjugate Chem.* **2008**, *19*, 1945−1950.
(27) Stevens, N. P. C.; Rooney, M. B.; Bond, A. M.; Feldberg, S. W. A Comparison of Simulated and Experimental Voltammograms Obtained for the [Fe(CN)6]3-/4- Couple in the Absence of Added Supporting Electrolyte at a Rotating Disk Electrode. *J. Phys. Chem. A* **2001**, *105*, 9085−9093.
(28) Rooney, M. B.; Coomber, D. C.; Bond, A. M. Achievement of Near-Reversible Behavior for the [Fe(CN)6]3-/4- Redox Couple Using Cyclic Voltammetry at Glassy Carbon, Gold, and Platinum Macrodisk Electrodes in the Absence of Added Supporting Electrolyte. *Anal. Chem.* **2000**, *72*, 3486−3491.
(29) Lee, C.; Anson, F. C. Inhibition of the electroreduction of $Fe(CN)_6^{3-}$ at microelectrodes in the absence of supporting electrolyte: Mediation of the inhibited reduction by methyl viologen. *J. Electroanal. Chem.* **1992**, *323*, 381−389.
(30) Bond, A. M.; Coomber, D. C.; Feldberg, S. W.; Oldham, K. B.; Vu, T. An Experimental Evaluation of Cyclic Voltammetry of Multicharged Species at Macrodisk Electrodes in the Absence of Added Supporting Electrolyte. *Anal. Chem.* **2001**, *73*, 352−359.
(31) Streeter, I.; Wildgoose, G. G.; Shao, L.; Compton, R. G. Cyclic voltammetry on electrode surfaces covered with porous layers: An analysis of electron transfer kinetics at single-walled carbon nanotube modified electrodes. *Sens. Actuators, B* **2008**, *133*, 462−466.
(32) Christian, G. D. *Analytical Chemistry*, 6th ed.; John Wiley & Sons, 2004; pp 111−113.
(33) USFDA. *Office of Foods and Veterinary Medicine*, 2015.
(34) Maalouf, R.; Fournier-Wirth, C.; Coste, J.; Chebib, H.; Saïkali, Y.; Vittori, O.; Errachid, A.; Cloarec, J.-P.; Martelet, C.; Jaffrezic-Renault, N. Label-free detection of bacteria by electrochemical impedance spectroscopy: comparison to surface plasmon resonance. *Anal. Chem.* **2007**, *79*, 4879.
(35) Mathebula, N. S.; Pillay, J.; Toschi, G.; Verschoor, J. A.; Ozoemena, K. I. Recognition of anti-mycolic acid antibody at self-assembled mycolic acid antigens on a gold electrode: a potential

https://dx.doi.org/10.1021/acsomega.9b03820
ACS Omega 2020, 5, 5762−5771

impedimetric immunosensing platform for active tuberculosis. *Chem. Commun.* **2009**, 3345−3347.
(36) Ionescu, R. E.; Jaffrezic-Renault, N.; Bouffier, L.; Gondran, C.; Cosnier, S.; Pinacho, D. G.; Marco, M.-P.; Sánchez-Baeza, F. J.; Healy, T.; Martelet, C. Impedimetric immunosensor for the specific label free detection of ciprofloxacin antibiotic. *Biosens. Bioelectron.* **2007**, *23*, 549−555.
(37) Ozoemena, K. I.; Mathebula, N. S.; Pillay, J.; Toschi, G.; Verschoor, J. A. Electron transfer dynamics across self-assembled N-(2-mercaptoethyl) octadecanamide/mycolic acid layers: impedimetric insights into the structural integrity and interaction with anti-mycolic acid antibodies. *Phys. Chem. Chem. Phys.* **2010**, *12*, 345−357.
(38) Guan, J.-G.; Miao, Y.-Q.; Zhang, Q.-J. Impedimetric biosensors. *J. Biosci. Bioeng.* **2004**, *97*, 219−226.
(39) Baur, J.; Gondran, C.; Holzinger, M.; Defrancq, E.; Perrot, H.; Cosnier, S. Label-free femtomolar detection of target DNA by impedimetric DNA sensor based on poly (pyrrole-nitrilotriacetic acid) film. *Anal. Chem.* **2010**, *82*, 1066−1072.
(40) Ašpergěr, S. Kinetics of the decomposition of potassium ferrocyanide in ultra-violet light. *Trans. Faraday Soc.* **1952**, *48*, 617−624.
(41) Zehavi, D.; Rabani, J. Pulse radiolysis of the aqueous ferro-ferricyanide system. 1. Reactions of OH, HO2, and O2-radicals. *J. Phys. Chem.* **1972**, *76*, 3703−3709.
(42) Zehavi, D.; Rabani, J. Pulse radiolysis of the aqueous ferro-ferricyanide system. II. Reactions of hydrogen atoms and hydrated electrons with ferrocyanide and ferricyanide ions. *J. Phys. Chem.* **1974**, *78*, 1368−1373.
(43) Le Caër, S.; Vigneron, G.; Renault, J. P.; Pommeret, S. First coupling between a LINAC and FT-IR spectroscopy: The aqueous ferrocyanide system. *Chem. Phys. Lett.* **2006**, *426*, 71−76.
(44) Risch, M.; Stoerzinger, K. A.; Regier, T. Z.; Peak, D.; Sayed, S. Y.; Shao-Horn, Y. Reversibility of Ferri-/Ferrocyanide Redox during Operando Soft X-ray Spectroscopy. *J. Phys. Chem. C* **2015**, *119*, 18903−18910.
(45) Goode, J. A.; Rushworth, J. V. H.; Millner, P. A. Biosensor regeneration: a review of common techniques and outcomes. *Langmuir* **2015**, *31*, 6267−6276.
(46) CDC. Cholera available at. https://www.cdc.gov/cholera/diagnosis.html (accessed on February 15, 2019).

https://dx.doi.org/10.1021/acsomega.9b03820
ACS Omega 2020, 5, 5762−5771